Supplementary materials

Analytical methods

Apatite, amphibole, and plagioclase analyses were porformed using an electron microprobe (JXA-8230) at the State Key Laboratory of Continental Dynamics, Northwest University, China. Samples were re-polished prior to electron probe microanalysis (EPMA) to remove any compositional modification induced by SEM electron-beam exposure, and subsequently carbon coated along with secondary standards to avoid variable light element X-ray attenuation. The instrument was operated at an accelerating voltage of 15 kV, beam current of 10 nA and beam diameter of 1 μm. Where possible, apatite crystals were analysed with the c-axis parallel to the plane of the mount. This routine limits the potential for time dependent variability in halogen X-ray counts during analysis (Stock et al., 2016, 2018), while maintaining reasonable precision for low-concentration elements (i.e., Cl). Count times were 20–30s for major elements and 30–90s for minor elements (120s for Cl and SO2 in apatite). Natural minerals and synthetic oxides were used as standards, including andradite for Si and Ca, rutile for Ti, corundum for Al, hematite for Fe, eskolaite for Cr, rhodonite for Mn, bunsenite for Ni, periclase for Mg, albite for Na, and K-feldspar for K. Matrix corrections were performed using the ZAF correction program supplied by the instrument manufacturer.

Rhyolite-MELTS fractionation modelling

Isobaric fractional crystallisation models were run using Rhyolite-MELTS (Gualda et al., 2012) to constrain the conditions of magma storage. We used the melt composition from partial melting experiments on a synthetic as the starting composition for our Rhyolite-MELTS models (melt C-3136 of Qian and Hermann, 2013), as distinguished by the similar partial melting condition with the lower crust of Sanjiang metallgenic belt.

Supplementary Figures

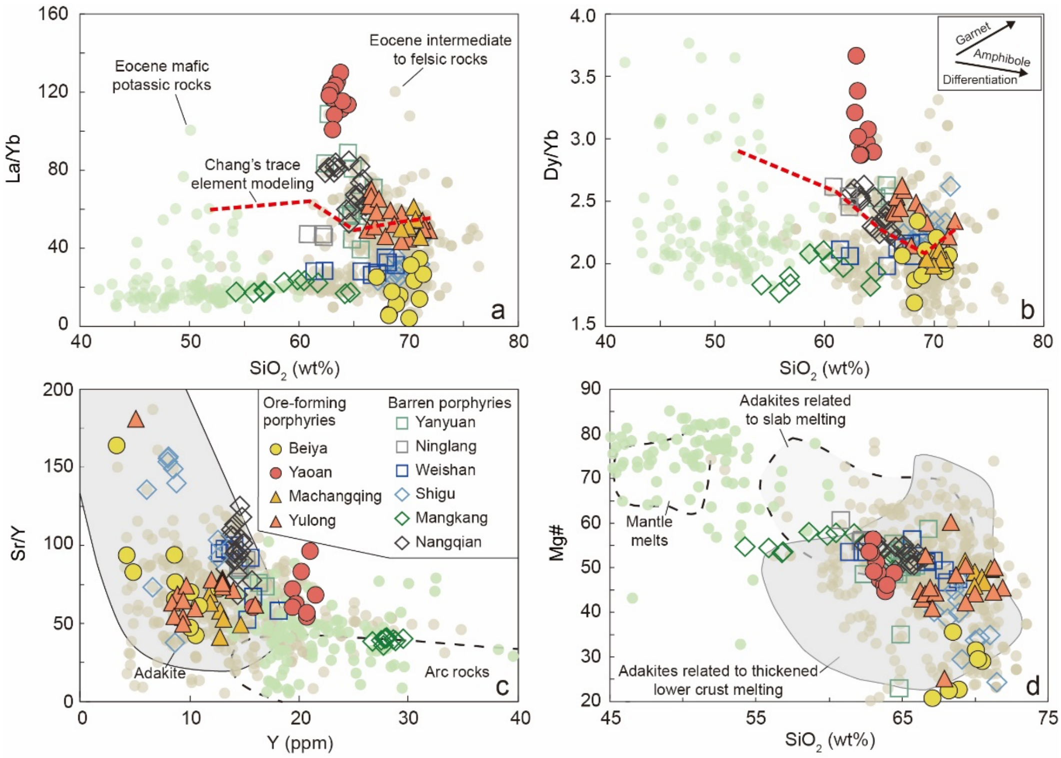

Supplementary Figure 1. Discrimination diagrams for Ore-forming and barren porphyries in the Sanjiang metallgenic belt. **a,** La/Yb ratios vs SiO_2 contents. **b,** Dy/Yb ratios vs SiO_2 contents. **c,** La/Yb ratios vs SiO_2 contents. **d,** Mg# vs SiO_2 contents. The red dashed lines in **a and b** represents the mafic rock fractionation modeling by Chang and and Audétat (2023). The adakite and arc rocks fields are according to Defant and Drummond (1990). Fields indicating mantle melt, adakites related to slab melting and lower-crustal melting are from Condie (2005), Wang et al. (2006) and Zheng et al. (2012).

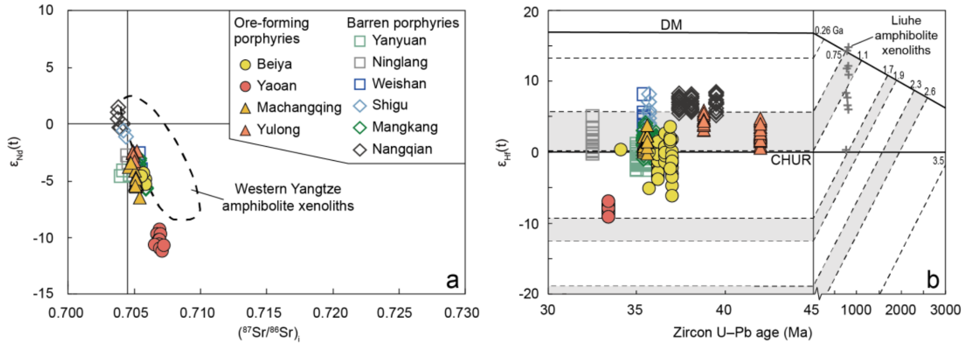

Supplementary Figure 2. Variation of **a,** $(^{87}Sr/^{86}Sr)_i$ vs $\varepsilon_{Nd}(t)$ and **b,** initial $\varepsilon_{Hf}(t)$ isotope values vs zircon U–Pb ages. The field for western Yangtze amphibolite xenoliths is from Deng et al. (1998), Zhao et al. (2004) and Zhou et al. (2017). CHUR, chondrite uniform reservoir; DM, depleted mantle. The values used for constructing the depleted mantle (DM) and crustal evolution reference lines are from Griffin et al. (2000, 2002). The light gray fields represent episodes of major juvenile crustal growth in the Yangtze craton (Sun et al., 2009). Neoproterozoic amphibolite xenoliths in the Liuhe area (Hou et al., 2017; Zhou et al., 2017)

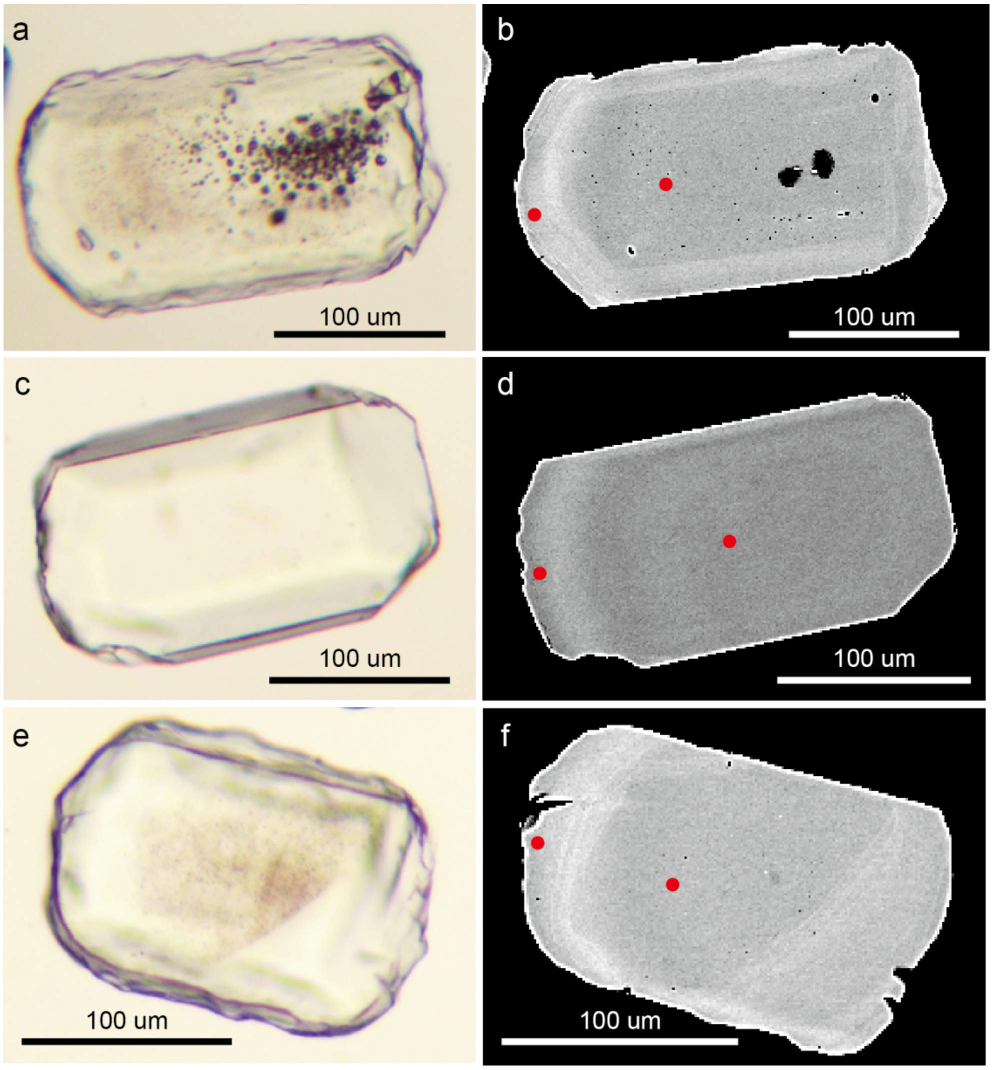

Supplementary Figure 3. (a, c, e) Photomicrograph and **(b, d, f)** backscattered electron images of apatites. The red spots show the positions of electron probe microanalysis (EPMA). All analyses of microphenocryst cores and rims are indistinguishable and show no evidence of re-equilibration with a volatile-saturated melt.

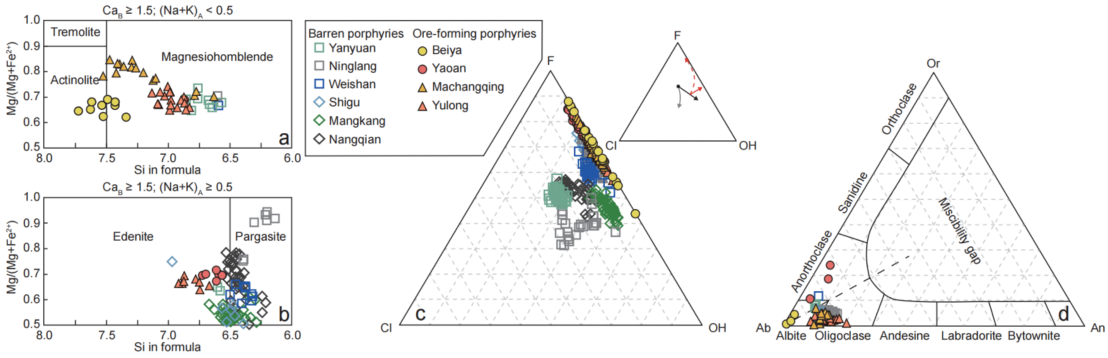

Supplementary Figure 4. a and b, Classification of amphibole (Leake et al., 1997). **c,** Ternary space of volatile compositions of apatites. **d,** Composition of feldspars in the An–Ab–Or ternary diagram (Smith, 1974). The representative ternary graph on the upper right illustrates theoretical apatite compositional trajectories for different crystallization scenarios. Apatite crystallization begins at the black point (see discussion of input parameters in the text). The continuous lines show apatite compositional evolution during H_2O-undersaturation fractional crystallization with Dc/m Cl ≈ 0.6 (grey continuous line) and Dc/m Cl ≈ 0.9 (black continuous line). The red lines show apatite compositional evolution during H_2O-saturation fractional crystallization under isobaric condition (0 wt% H_2O loss; red continuous line) and polybaric condition (0.18 wt% H_2O loss; red dotted line), after 40% crystallization under H_2O-undersaturated condition. Amphiboles and apatites are from ore-forming and barren adakite-like porphyries in Sanjiang metallogenic belt.

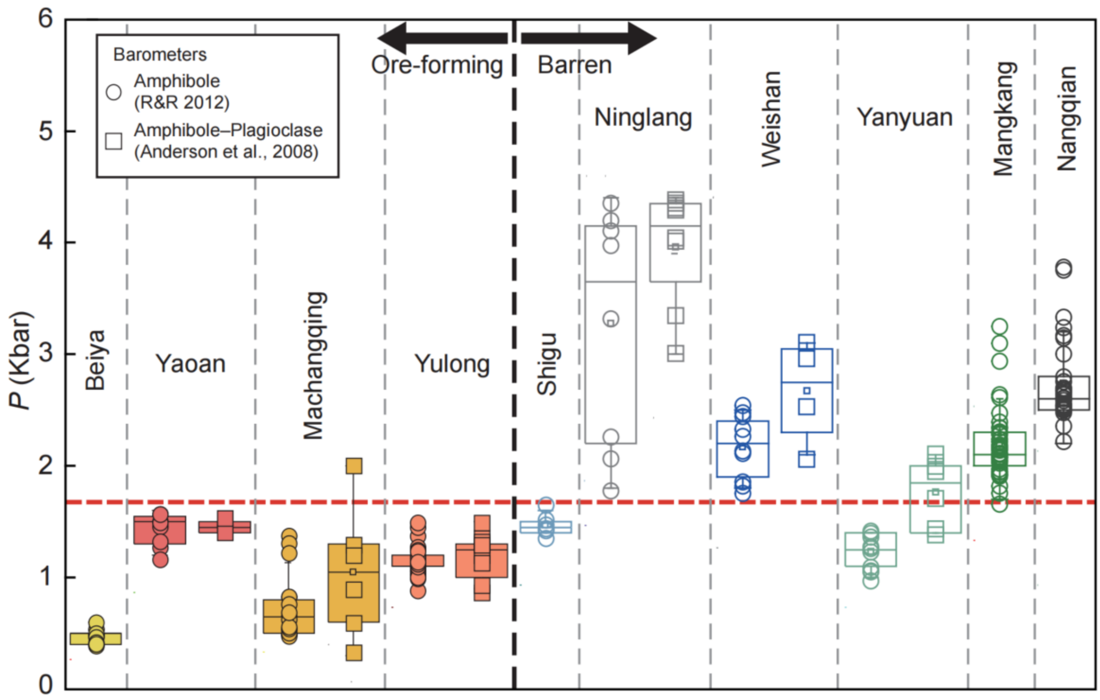

Supplementary Figure 5. Box and whisker plots of comparison of different barometer results. The dots represent the results calculated by amphibole-only barometer (Ridolfi and Renzulli, 2012), and the squares represent the results calculated by amphibole–plagioclase barometer (Anderson et al., 2008). Boxes show first to third quartile range with bars showing extremes of data (excluding any outliers). Long and short lines in box show square and mean value, respectively. The points outside boxes represent their extremum values.

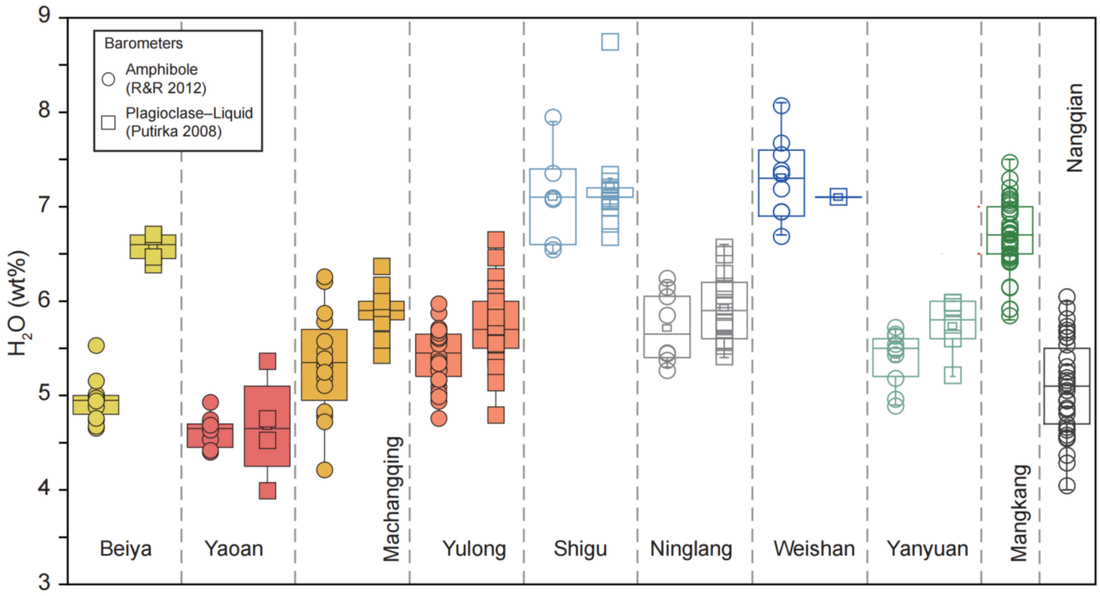

Supplementary Figure 6. Box and whisker plots of comparison of different hygrometer results. The dots represent the results calculated by amphibole-only hygrometer (Ridolfi and Renzulli, 2012), and the squares represent the results calculated by plagioclase–liquid hygrometer (Putirka et al., 2008). The box and whisker meanings are the same as those in Supplementary Figure 5.

Supplementary References

Anderson, J.L., Barth, A.P., Wooden, J.L., and Mazdab, F. (2008). Thermometers and thermobarometers in granitic systems. Reviews in mineralogy and geochemistry, 69(1), 121–142.

Chang, J. and Audétat, A. (2023) Post-subduction porphyry Cu magmas in the Sanjiang region of southwestern China formed by fractionation of lithospheric mantle–derived mafic magmas. Geology, 51(1), 64–68.

Condie, K.C. (2005). TTGs and adakites: are they both slab melts? Lithos, 80: 33–44.

Defant, M.J., Drummond, M.S. 1990. Derivation of some modern arc magmas by melting of young subducted lithosphere. Nature, 347: 662–665.

Deng, W.M., Huang, X., and Zhong, D. L. (1998). Petrological characteristics and genesis of Cenozoic alkali-rich porphyry in West Yunnan, China. Scientia Geologica Sinica, 33, 412–425 (in Chinese with English abstract).

Griffin, W.L., Wang, X., Jackson, S.E., Pearson, N.J., O'Reilly, S.Y., Xu, X., and Zhou, X. (2002). Zircon chemistry and magma mixing, SE China: In-situ analysis of Hf isotopes, Tonglu and Pingtan igneous complexes. Lithos, 61, 237–269.

Griffin, W.L., Pearson, N.J., Belousova, E., Jackson, S.V., Van Achterbergh, E., O’Reilly, S.Y., and Shee, S.R. (2000). The Hf isotope composition of cratonic mantle: LAM–MC–ICPMS analysis of zircon megacrysts in kimberlites. Geochimica et Cosmochimica Acta, 64, 133–147.

Gualda, G.A.R., Ghiorso, M.S., Lemons, R.V., and Carley, T.L. (2012). Rhyolite-MELTS: a modified calibration of MELTS optimized for silica-rich, fluid-bearing magmatic systems. Journal of Petrology, 53(5), 875–890.

Hou, Z.Q., Zhou, Y., Wang, R., Zheng, Y.C., He, W.Y., Zhao, M., Evans, N.J., and Weinberg, R.F. (2017). Recycling of metal-fertilized lower continental crust: Origin of non-arc Au-rich porphyry deposits at cratonic edges. Geology, 45(6), 563–566.

Leake, B.E., Woolley, A.R., Arps, C.E.S., Birch,W.D., Charles Gilbert, M., Grice, J.D., Hawthorne, F.C., Kato, A., Kisch, H.J., Krivovichev, V.G., Linthout, K., Laird, J., Mandarino, J.A., Maresch,W.V., Nickel, E.H., Rock, N.M.S., Schumacher, J.C., Simith, D.C., Stephenson, N.C.N., Ungaretti, L., Whittaker, E.J.W., and Guo, Y.Z. (1997). Nomenclature of amphiboles; report of the Subcommittee on Amphiboles of the International Mineralogical Association Commission on new minerals and mineral names. The Canadian Mineralogist, 35(1), 219–246.

Putirka, K.D. (2008). Thermometers and barometers for volcanic systems. Reviews in mineralogy and geochemistry, 69(1), 61–120.

Qian, Q., and Hermann, J. (2013). Partial melting of lower crust at 10–15 kbar: constraints on adakite and TTG formation. Contributions to Mineralogy and Petrology, 165(6), 1195–1224.

Ridolfi, F., and Renzulli, A. (2012). Calcic amphiboles in calc-alkaline and alkaline magmas: thermobarometric and chemometric empirical equations valid up to 1,130 °C and 2.2 GPa. Contributions to Mineralogy and Petrology, 163(5), 877–895.

Smith, J.F. (1974). Feldspar Minerals. Berlin: Springer.

Stock, M.J., Humphreys, M.C., Smith, V.C., Isaia, R., and Pyle, D.M. (2016). Late-stage volatile saturation as a potential trigger for explosive volcanic eruptions. Nature Geoscience, 9, 249–254.

Stock, M.J., Humphreys, M.C., Smith, V.C., Isaia, R., Brooker, R.A., and Pyle, D.M. (2018). Tracking volatile behaviour in sub-volcanic plumbing systems using apatite and glass: insights into pre-eruptive processes at Campi Flegrei, Italy. Journal of Petrology, 59(12), 2463–2492.

Sun, W.H., Zhou, M.F., Gao, J.F., Yang, Y.H., Zhao, X.F., and Zhao, J.H. (2009). Detrital zircon U–Pb geochronological and Lu–Hf isotopic constraints on the Precambrian magmatic and crustal evolution of the western Yangtze Block, SW China. Precambrian Research, 172, 99–126.

Wang, Q., Xu, J.F., Jian, P., Bao, Z.W., Zhao, Z.H., Li, C.F., Xiong, X.L., and Ma, J.L. (2006). Petrogenesis of adakitic porphyries in an extensional tectonic setting, Dexing, South China: implications for the genesis of porphyry copper mineralization. Journal of Petrology, 47, 119–144.

Zhao, X., Yu, X.H., Mo, X.X., Zhang, J., and Lu, B.X. (2004). Petrological and geochemical characteristics of Cenozoic alkali-rich porphyries and xenoliths hosted in western Yunnan province. Geoscience, 18, 217–228 (in Chinese with English abstract).

Zheng, Y.C., Hou, Z.Q., Li, W., Liang, W., Huang, K.X., Li, Q.Y., Sun, Q.Z., Fu, Q., and Zhang, S. (2012). Petrogenesis and geological implications of the Oligocene Chongmuda–Mingze adakite-like intrusions and their mafic enclaves, Southern Tibet. Journal of Geology, 120, 647–669.

Zhou, Y., Hou, Z.Q., Zheng, Y.C., Xu, B., Wang, R., and Luo, C.H. (2017). Granulite xenoliths in Liuhe area: evidence for composition and genetic mechanism of the lower crust from the Neoproterozoic to Cenozoic. Acta Petrologica Sinica, 33, 2143–2160 (in Chinese with English abstract).